Internalization of Indium-111 into Human Neuroendocrine Tumor Cells after Incubation with Indium-111-DTPA-D-Phe^1-Octreotide

Peter Andersson, Eva Forssell-Aronsson, Viktor Johanson, Bo Wängberg, Ola Nilsson, Martha Fjälling and Håkan Ahlman
Departments of Radiation Physics, Surgery and Pathology, Göteborg University, Sahlgrenska University Hospital, Göteborg, Sweden; and Division of Nuclear Medicine, Sahlgrenska University Hospital, Göteborg, Sweden

Neuroendocrine tumor cells frequently overexpress somatostatin receptors at their cell surfaces. To evaluate the possibility of using the somatostatin analog ^{111}In-DTPA-D-Phe^1-octreotide for radiation therapy, we studied the binding and subsequent internalization of ^{111}In into three types of cultured human neuroendocrine tumor cells. **Methods:** Primary cultures of gastric carcinoid, midgut carcinoid and glucagonoma cells were incubated with ^{111}In-DTPA-D-Phe^1-octreotide and cell-surface bound, internalized and released ^{111}In activity was measured. Electron microscopic autoradiography was also performed. **Results:** All three cell types specifically (80%–95%) bound ^{111}In-DTPA-D-Phe^1-octreotide and internalized ^{111}In. After 1 hr pulse incubation with ^{111}In-DTPA-D-Phe^1-octreotide, there was an initial decrease in intracellular ^{111}In to about 50% during the subsequent 6-hr incubation. Almost no further release was observed during the remaining 18–42 hr studied. Autoradiography showed that the internalized ^{111}In was found in the cytoplasm and nucleus in the midgut carcinoid cells. **Conclusion:** Indium-111 DTPA-D-Phe^1-octreotide might be useful for radiation therapy of patients with surgically incurable tumors having high somatostatin receptor densities.

Key Words: indium-111-octreotide; somatostatin receptors; neuroendocrine tumors

J Nucl Med 1996; 37:2002–2006

Somatostatin is a naturally occurring peptide known to suppress pituitary hormone secretion as well as secretion from many endocrine and exocrine cell types in the gastrointestinal tract (*1*). In most systems, somatostatin exerts an inhibitory effect on several cell functions e.g., secretion of biogenic amines, peptide hormones and growth factors (*2–4*). An increased number of somatostatin receptors has been found in neuroendocrine tumors (*5,6*). Due to a very short half-time (<3 min) in vivo, the clinical value of somatostatin is limited, while a more stable synthetic somatostatin analog, octreotide, is widely used for symptomatic treatment of patients with neuroendocrine tumors (*1*).

Clinically ^{111}In-DTPA-D-Phe^1-octreotide is used for scintigraphic localization of neuroendocrine tumors (*7–12*). In patients with carcinoids or endocrine pancreatic tumors, very high tumor-to-normal tissue ^{111}In activity concentration ratios (50–1500) have been found after injection of ^{111}In-DTPA-D-Phe^1-octreotide (*13*), indicating therapeutic potential for radiolabeled octreotide. This possibility has, in fact, already been tried in individual patients with interesting preliminary results (*14*). Since ^{111}In emits Auger electrons with a range less than the dimension of a cell (*15*), a prerequisite for efficient radiation therapy is internalization of ^{111}In into the tumor cells. Although accumulation or long-lasting binding of ^{111}In in neuroendocrine tumors is evident from somatostatin receptor scintigraphy (*14*), the exact localization of ^{111}In at the subcellular level is not known. Internalization of somatostatin together with its receptors have been proposed for several cell types e.g., pancreatic acinar cells (*16*) and rat pituitary cells (*17*), but no such studies have previously been performed on human neuroendocrine tumor cells.

The aim of the present investigation was to study the binding, possible internalization and subsequent release of ^{111}In after incubation of primary cultures of human glucagonoma and carcinoid cells with ^{111}In-DTPA-D-Phe^1-octreotide.

MATERIALS AND METHODS

Tumor Cell Cultures

Tumor tissue from three patients with midgut carcinoid, gastric carcinoid and glucagonoma, respectively, were obtained at surgery and processed for tissue culture. All tumors were receptor-positive at ^{111}In-DTPA-D-Phe^1-octreotide scintigraphy. Tumor tissue was harvested from liver metastases (carcinoids) or primary tumor (glucagonoma).

The preparation and characterization of long-term carcinoid tumor-cell cultures have been described previously (*18*). In brief, cell suspensions were prepared and tumor cells were seeded onto collagen-coated, tissue-culture plates at a density of 10^5–10^6 cells per well and incubated in RPMI 1640 medium (Northumbria Biologicals, Cramlington, U.K.) supplemented with 4% fetal calf serum.

The experiments were performed on tumor cells after 2 wk in primary culture. During this period, the cultures never grew to confluence. In cultures from all three tumors, a minority of stroma cells (<20%) were present beside the tumor cells. Tumor cells were easily identified by phase-contrast microscopy and shown to be immunocytochemically positive for serotonin, histidine decarboxylase and glucagon, respectively. Before conducting the experiments, the maintenance media were discarded and the cells were washed once with DPBS (Dulbecco phosphate-buffered saline).

Radiopharmaceutical

Radiolabeling of DTPA-D-Phe^1-octreotide with ^{111}In was performed according to the manufacturer's instructions (Mallinckrodt Medical B.V, The Netherlands) but with a specific activity of 240 MBq ^{111}In per 10 μg DTPA-D-Phe^1-octreotide. Chromatography of the radiopharmaceutical was performed using instant thin layer chromatography (ITLC-SG, Gelman Instrument Company, MI) with sodium-citrate (0.1 *M*, pH 5) as the mobile phase. The fraction of peptide-bound ^{111}In was more than 98%.

Received Sept. 25, 1995; revision accepted Apr. 10, 1996.
For correspondence or reprints contact: Peter Andersson, Department of Radiation Physics, Göteborg University, Sahlgrenska University Hospital, S-413 45 Göteborg, Sweden.

Experimental Studies

The binding of ^{111}In-DTPA-D-Phe^1-octreotide to tumor cells and possible subsequent internalization of ^{111}In were studied by two different protocols. Radioactivity still bound to the cells after trypsinization was assumed to represent ^{111}In internalized into tumor cells, while ^{111}In detached by trypsin was assumed to represent cell surface-bound ^{111}In as shown by binding studies and electron microscope autoradiography for other radiolabeled peptides, including an octapeptide (CCK-8) (*19*).

Protocol 1. In the binding studies, wells (duplicate) with tumor cells were incubated with 150 μl RPMI 1640 medium supplemented with 1% bovine serum albumin (BSA) containing about 80 kBq ^{111}In-DTPA-D-Phe^1-octreotide, corresponding to 10 n*M* of octreotide, at 37°C for 1–6 hr. The medium was then removed, and the cells were washed rapidly three times with 1 ml Ca- and Mg-free DPBS. To remove surface-bound ^{111}In-DTPA-D-Phe^1-octreotide from the cell surface and to detach the cells from the wells, the cells were incubated with 0.5 ml of trypsin solution (0.05% trypsin) at 37°C for 15 min. The cells were transferred with 1 ml DPBS into plastic tubes and centrifuged at 900× g for 5 min and washed once again with DPBS. The amount of surface-bound and internalized ^{111}In was determined by radioactivity measurements of the supernatants and the pellets, respectively, with a gamma spectrometer containing a NaI(Tl) well crystal and a single-channel, pulse-height analyzer. Correction was made for background, radioactive decay and nonspecific binding as described below.

Protocol 2. In the pulse incubation studies, wells (duplicate) with tumor cells were incubated at 37°C for 1 hr with 150 μl RPMI 1640 medium supplemented with 1% BSA containing about 80 kBq ^{111}In-DTPA-D-Phe^1-octreotide, corresponding to 10 n*M* octreotide. The medium was removed, and the cells were washed rapidly three times with 1 ml DPBS and further incubated with RPMI 1640 medium at 37°C. After 1–48 hr, the medium was removed and the cells were trypsinized and washed as previously described. The amounts of surface-bound, internalized and subsequently released ^{111}In were determined by radioactivity measurements with the gamma spectrometer of the supernatants, pellets and medium, respectively. Correction was made for background, radioactive decay and nonspecific binding as described below.

For gastric carcinoid cells, the fraction of trichloroacetic acid (TCA) precipitable activity in the pellet was determined after adding 10% TCA to the pellet, which was first centrifuged (1200× g for 10 min) and then measured for radioactivity.

To determine the specificity of the measured binding, internalization and subsequent release of ^{111}In, duplicate control wells were processed as described above, but the incubation was performed in the presence of a 500-fold excess of unlabeled octreotide. These results were then used for correction for nonspecific binding.

Electron Microscope Autoradiography

Wells with midgut carcinoid cells were incubated at 37°C for 4 hr with 150 μl of RPMI 1640 medium supplemented with 1% BSA containing about 80 kBq ^{111}In-DTPA-D-Phe^1-octreotide, corresponding to 10 n*M* octreotide. Paired control wells were treated similarly but with the addition of a 500-fold excess of unlabeled octreotide. After incubation, the medium was removed and the cells washed rapidly three times with 1 ml DPBS and further incubated with RPMI medium at 37°C. After 6 hr, the medium was removed and the cells were trypsinized, centrifuged and washed as previously described.

The pellets, containing the cells, were fixed in 2.5% glutaraldehyde in 0.05 *M* sodium cacodylate at 4°C for 1 hr and postfixed in 1% osmium tetroxide in 0.1 *M* sodium cacodylate at room temperature for 1 hr. After graded dehydration in ethanol, the cell pellets were embedded in Agar 100 (Agar Aids, U.K.). Ultrathin sections (~50 nm), picked up on Formvar-coated copper grids, were contrasted with uranyl acetate and lead citrate and carbon-coated by vacuum evaporation. Ilford L4 emulsion (Ilford Ltd., U.K.) was applied with a wire loop (*20*). After exposure for 1 wk at 4°C, the preparations were developed in Kodak D19 for 1.5 min and fixed in Kodak F24 for 5 min. Autoradiographs were examined and photographed in a Philips EM 400 electron microscope. Silver grains were counted over the cytoplasm and nucleus of midgut carcinoid cells and stroma cells. Cell profile areas were estimated by morphometry (point counting), and relative silver grain density was calculated over cytoplasm and nucleus (*21*).

TABLE 1
Tumor-to-Blood Ratios (T/B) and Indium-111 Activity Concentration (C) Postintravenous Injection of Indium-111-DTPA-D-Phe^1-Octreotide

Tumor biopsy	T/B	C (%IA/g)	Time after injection (d)
Glucagonoma			
Primary tumor	910	0.059	3
Liver metastasis	650	0.042	3
Midgut carcinoid			
Primary tumor	150	0.008	7
Liver metastasis	400	0.020	7
Liver metastasis	470	0.024	7
Liver metastasis	650	0.033	7
Gastric carcinoid			
Primary tumor	71	0.017	1
Lymph node metastasis	190	0.047	1
Liver metastasis	150	0.035	1
Liver metastasis	180	0.044	1
Liver metastasis	210	0.051	1

Indium-111 Concentration in Tumor Samples

Each of the three patients received 10–20 μg ^{111}In-DTPA-D-Phe^1-octreotide (190–350 MBq) by intravenous injection 24–168 hr before surgery. Before routine histopathological examination, the surgical specimens together with blood samples drawn during surgery were weighed, and the ^{111}In activity was measured with the gamma counter. Correction was made for background and radioactive decay. Tumor-to-blood ^{111}In activity concentration ratios (T/B) were calculated for the histologically-proven tumor lesions (*13,22*).

RESULTS

The activity concentration of ^{111}In in tumor tissues harvested for cell culture studies were measured by the gamma counter after excision and compared with the corresponding values in blood. The calculated T/B ratios were thus 910 (glucagonoma), 400–650 (midgut carcinoid) and 150–210 (gastric carcinoid) (Table 1).

Human glucagonoma and carcinoid cells in primary culture bound ^{111}In specifically during incubation with ^{111}In-DTPA-D-Phe^1-octreotide at 37°C. Concomitant incubation with excess of unlabeled octreotide resulted in inhibited binding of ^{111}In (glucagonoma cells >95%, midgut carcinoid cells >90% and gastric carcinoid cells ~80%).

The three different tumor cell cultures bound ^{111}In to a varying degree: the glucagonoma cell culture bound about 5 and 40 times more ^{111}In (surface bound + internalized) than the midgut carcinoid cell and the gastric carcinoid cell culture, respectively (Fig. 1). The difference in cell density between cultures, estimated by phase contrast microscopy, did not differ more than by a factor of two. The amount of internalized ^{111}In

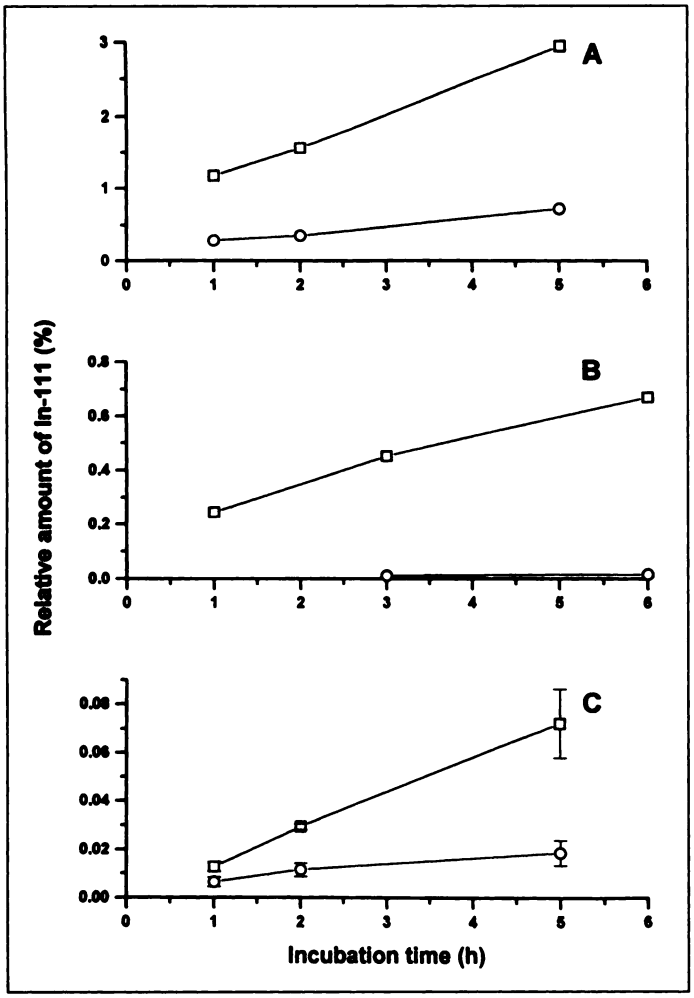

FIGURE 1. Surface-bound (circles) and internalized (squares) ^{111}In versus time of incubation with ^{111}In-DTPA-D-Phe^{1}-octreotide. (A) Glucagonoma cells, (B) midgut carcinoid cells and (C) gastric carcinoid cells. Error bars show ±1 s.d. In most data points, the error bars are smaller than the symbols.

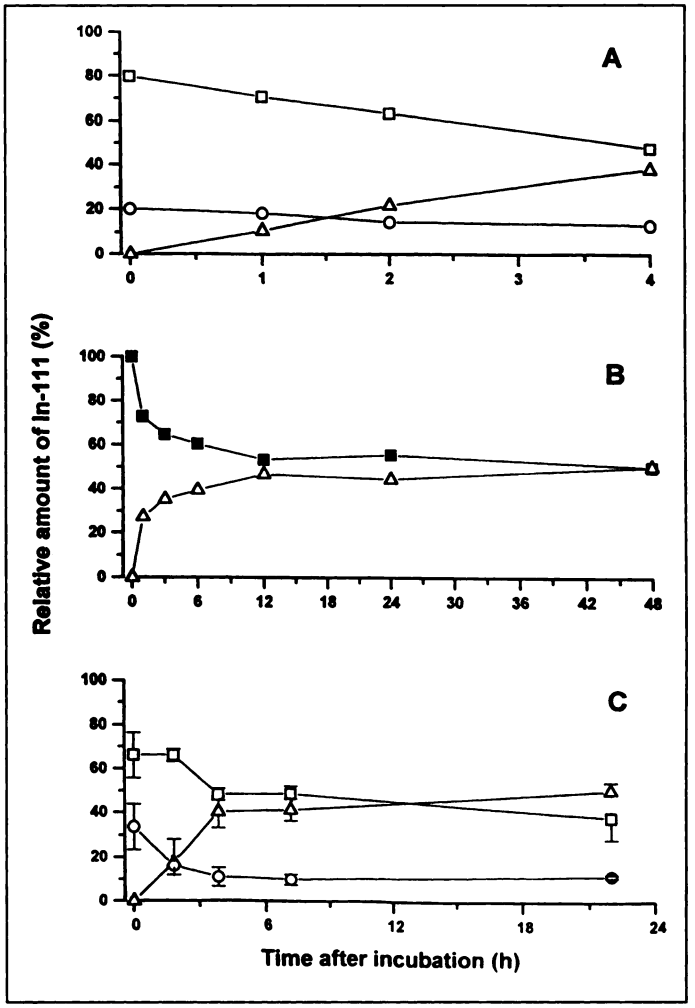

FIGURE 2. Surface-bound (circles), internalized (open squares), released (triangles) and cell-bound (closed squares) ^{111}In versus time after 1-hr incubation with ^{111}In-DTPA-D-Phe^{1}-octreotide. (A) Glucagonoma cells, (B) midgut carcinoid cells and (C) gastric carcinoid cells. Error bars show ±1 s.d. In most data points, the error bars are smaller than the symbols.

increased markedly with incubation time, while surface-bound ^{111}In increased to a small degree in both glucagonoma cells and carcinoid cells (Fig. 1). The internalized ^{111}In in gastric carcinoid cells was TCA-precipitable to 60%.

The cellular redistribution of ^{111}In after 1 hr pulse incubation with ^{111}In-DTPA-D-Phe^{1}-octreotide is shown in Figure 2. The amount of internalized ^{111}In decreased, and the amount of ^{111}In released into the medium increased with time. After an initial decrease of intracellular ^{111}In in midgut carcinoid cells, about 50% of the internalized ^{111}In was maintained intracellularly with no further redistribution during the period of study (Fig. 2B). A similar pattern was seen for the gastric carcinoid cells (Fig. 2C). The glucagonoma cells were only studied for 4 hr but showed a similar redistribution pattern during this time (Fig. 2A). The amount of surface-bound ^{111}In was studied in glucagonoma cells and gastric carcinoid cells and showed a slow decrease over time (Fig. 2A, C).

The subcellular distribution of ^{111}In in the midgut carcinoid cells was studied by electron microscope autoradiography (Fig. 3). The grain density was low; the silver grains were mainly distributed over the cytoplasm but also over the nucleus (Table 2). The nucleus in midgut carcinoid cells represented 11% of the total cell volume, estimated by morphometry, and the calculated grain density was thus about three times higher over the cytoplasm than over the nucleus. No grains were found over the surrounding stroma cells, background or over tumor cells from control incubations with excess of unlabeled octreotide.

DISCUSSION

The present study provides the first evidence of internalization of ^{111}In into human carcinoid and glucagonoma tumor cells in primary culture after incubation with ^{111}In-DTPA-D-Phe^{1}-octreotide. Primary culture of neuroendocrine tumor cells is performed under conditions similar to culture of neurons. It has advantages for the study of authentic tumor cell properties but is limited by deterioration of cells within a few weeks (reflected by decreasing hormone production) leading to limited access of cells for repeated studies (*4*).

The binding and internalization of ^{111}In was no more than 80% inhibited by excess of octreotide, indicating that binding and internalization were specific. The binding and internalization of ^{111}In was higher for glucagonoma cultures than for carcinoid cultures, probably due to tumor-specific factors such as somatostatin receptor subtypes and their densities and the rate of intracellular accumulation of ^{111}In. These observed differences between the ^{111}In binding in vitro agreed with the differences in ^{111}In binding in vivo in the surgical specimens (Table 1). It is unlikely that changes in the binding kinetics for the tumor cells studied were due to proliferative effects since primary cultures of human neuroendocrine tumor cells have a

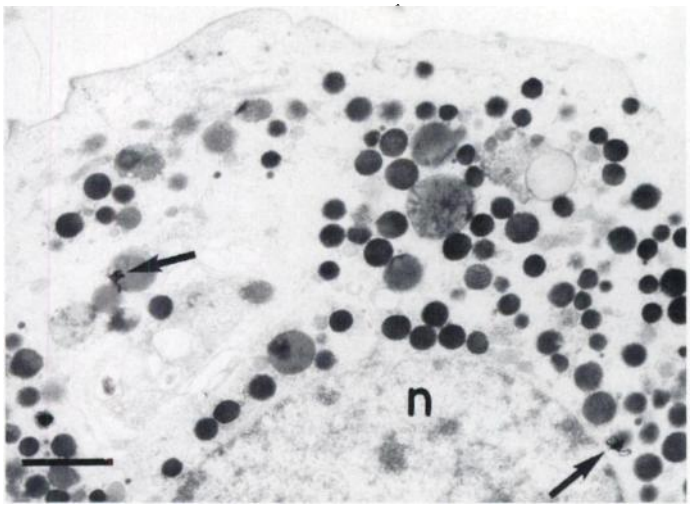

FIGURE 3. Electron microscopical autoradiography of ^{111}In in human cultured midgut carcinoid cells after 4-hr incubation with ^{111}In-DTPA-D-Phe^1-octreotide followed by 6-hr incubation in ^{111}In-free medium. Two silver grains marked by arrows are located over the cytoplasm in the tumor cell. **n** = nucleus. Bar = 1 μm.

low proliferation rate (*2,4*). We previously cultured such cells for 4 days without any significant change in DNA content. When studied over 14 days, 10 n*M* octreotide had no significant antiproliferative effects (*4*).

After pulse incubation with ^{111}In-DTPA-D-Phe^1-octreotide, the accumulated intracellular ^{111}In was released from the tumor cells into the medium following a similar time course in all three tumor types. In two tumor cell cultures, studied for more than 6 hr, there appeared to be no further redistribution of ^{111}In after this time. This indicates that ^{111}In was associated with intracellular structures, as was also suggested from the TCA studies in gastric carcinoid cells.

Electron microscope autoradiography showed that ^{111}In was internalized into midgut carcinoid cells. The internalization was highly specific, as no silver grains at all were detected over stroma cells, background or over tumor cells incubated with an excess of unlabeled octreotide. The estimated ratio of grain density between the cytoplasm and the nucleus was 3:1. A high nuclear accumulation of ^{111}In would be advantageous for radiation therapy.

The radionuclides that decay by Auger-electron-emitting processes (e.g., ^{111}In and ^{125}I) are highly radiotoxic if incorporated into DNA (*23–24*), or if they are located elsewhere in the nucleus (*25–26*). The experiment of Warters et al. (*27*) showed that 60 disintegrations of ^{125}I per nucleus (in iododeoxyuridine) gave a 50% cell death in V-79 cells. To obtain a similar effect by ^{125}I at the cell surface, as many as 19600 disintegrations were needed. Our results show that ^{111}In was located intracellularly, which is a prerequisite for radiobiological effect due to the short range of the Auger electrons.

TABLE 2
Intracellular Distribution of Indium-111 after Incubation with Indium-111-Octreotide Studied by Electron Microscopical Autoradiography

Type of cells	Number of cell profiles studied	Number of grains over cytoplasm	Number of grains over nucleus
Tumor cells*	45	71	3
Tumor cell controls†	39	0	0
Stroma cells‡	17	0	0
Stroma cell controls§	16	0	0

*Midgut carcinoid cells incubated with ^{111}In-labeled octreotide.

†Midgut carcinoid cells incubated with ^{111}In-labeled octreotide together with excess of unlabeled octreotide.

‡Stroma cells incubated with ^{111}In-labeled octreotide.

§Stroma cells incubated with ^{111}In-labeled octreotide together with excess of unlabeled octreotide.

CONCLUSION

The present study demonstrates that human neuroendocrine tumor cells in culture specifically bound and internalized ^{111}In after incubation with ^{111}In-DTPA-D-Phe^1-octreotide. Autoradiography showed that ^{111}In was distributed both in the cytoplasm and in the nucleus. In pulse incubation experiments, the decline of intracellular ^{111}In concentration was most prominent during the first 6 hr and seemed to remain stable thereafter. Our results therefore emphasize the therapeutical potential of ^{111}In-DTPA-D-Phe^1-octreotide for patients with neuroendocrine tumors with high tumor/(normal tissue) ^{111}In activity concentration over time (*13*). Further studies of the intracellular localization of ^{111}In in different types of neuroendocrine tumors need to be compared with that of normal tissues as a basis for potential radiation therapy.

ACKNOWLEDGMENTS

We thank Sandoz for supplying the octreotide. We also thank Gunnel Bokhede, Ann-Christin Illerskog, Yvonne Josefsson and Anneli Wigander in the Department of Anatomy and Cell Biology for technical assistance.

This work was supported by Swedish National Cancer Society grants 3427, 2998, Swedish MRC grant 5220, by the Swedish Medical Society, Sahlgrenska University Hospital Research Funds and the A. Gabrielsson Research Foundation.

REFERENCES

1. Gordon P, Comi RJ, Maton PN, Go VLM. Somatostatin and somatostatin analog (SMS 201-995) in treatment of the pituitary and gastrointestinal tract and non-neoplastic diseases of the gut. *Ann Intern Med* 1989;110:35–52.
2. Nilsson O, Wängberg B, Kölby L, Schultz G, Ahlman H. Expression of transforming growth factor alpha and its receptor in human neuroendocrine tumors. *Int J Cancer* 1995;60:645–651.
3. Nilsson O, Wängberg B, Theodorsson E, Skottner A, Ahlman H. Presence of IGF in human midgut carcinoid tumors—an autorine regulation of carcinoid tumor growth? *Int J Cancer* 1992;51:195–203.
4. Wängberg B, Nilsson O, Theodorsson E, Dahlström A, Ahlman H. The effect of a somatostatin analog in the release of hormones from human midgut carcinoid tumor cells. *Br J Cancer* 1991;64:23–28.
5. Reubi JC, Häckl W, Lamberts SWJ. Hormone-producing gastrointestinal tumors contain a high density of somatostatin receptors. *J Clin Endocrinol Metab* 1987;65: 1127–1134.
6. Reubi JC, Kvols LK, Waser B, et al. Detection of somatostatin receptors in surgical percutaneous needle biopsy of carcinoids and islet carcinomas. *Cancer Res* 1990;50: 5969–5977.
7. Krenning EP, Kwekkeboom DJ, Bakker WH, et al. Somatostatin receptor scintigraphy with [^{111}In-DTPA-D-Phe^1]- and [^{123}I-Tyr^3]-octreotide: the Rotterdam experience with more than 1000 patients. *Eur J Nucl Med* 1993;20:716–731.
8. Ahlman H, Wängberg B, Tisell LE, Nilsson O, Fjälling M, Forssell-Aronsson E. Clinical efficacy of ^{111}In-DTPA-Phe^1-octreotide scintigraphy in patients with midgut carcinoid tumors and evaluation of intraoperative scintillation detection. *Br J Surg* 1994;81:1144–1149.
9. Ahlman H, Tisell LE, Wängberg B, Nilsson O, Fjälling M, Forssell-Aronsson E. Somatostatin receptor imaging in patients with neuroendocrine tumors: preoperative and postoperative scintigraphy and intraoperative use of a scintillation detection. *Semin Oncol* 1994;21:21–28.
10. Maini CL, Tofani A, Sciuto R, Carapella C, Cioffi R, Crecco M. Somatostatin receptors in meningiomas: a scintigraphic study using ^{111}In-DTPA-D-Phe^1-octreotide. *Nucl Med Commun* 1993;14:550–558.
11. Kwekkeboom DK, van Urk H, Pauw BKH, et al. Octreotide scintigraphy for the detection of paragangliomas. *J Nucl Med* 1993;34:873–878.
12. Dörr U, Frank-Raue K, Raue F, et al. The potential value of somatostatin receptor scintigraphy in medullary thyroid carcinoma. *Nucl Med Commun* 1993;14:439–445.
13. Forssell-Aronsson E, Fjälling M, Nilsson O, Tisell LE, Wängberg B, Ahlman H. ^{111}In activity concentration in human tissue samples after i.v. injection of ^{111}In-DTPA-Phe^1-octreotide. *J Nucl Med* 1995;36:7–12.

14. Krenning EP, Kooij DPM, Bakker WH, et al. radiotherapy with a radiolabeled somatostatin analog [^{111}In-DTPA-Phe^1]-octreotide. In: Wiedermann B, Kvols LK, Arnold R, Rieken EO, eds. Molecular and cell biological aspects of gastroenteropancreatic. *Ann NY Acad Sci* 1994;733:496–506.
15. McLean JR, Blakey DH, Douglas GR, Bayley J. The Auger electron dosimetry of indium-111 in mammalian cells in vitro. *Radiat Res* 1989;119:205–218.
16. Viguerie N, Esteve JP, Susini C, Vaysse N, Ribet A. Processing of receptor-bound somatostatin: internalization and degradation by pancreatic acini. *Am J Physiol* 1987;252:G535–G542.
17. Morel G. Internalization and nuclear localization of peptide hormones. *Biochem Pharmacol* 1994;47:63–76.
18. Ahlman H, Åhlund L, Nilsson O, Skolnik G, Theodorsson E, Dahlström A. Carcinoid cells in long-term culture: release of serotonin but not of tachykinins on stimulation with adrenoreceptor agonists. *Int J Cancer* 1988;42:506–511.
19. Williams JA, Bailey AC, Roach E. Temperature dependence of high-affinity CCK receptor binding and CCK internalization in rat pancreatic acini. *Am Physiol Soc* 1988;254:513–521.
20. Caro LG, Van Tubberghen RP, Roll JA. High-resolution autoradiography. I. Methods. *J Cell Biol* 1962;15:173–188.
21. Weibel ER. Practical methods for biological morphometry. In: *Stereological methods*, vol. 1. London: Academic Press; 1979:101.
22. Wängberg B, Forssell-Aronsson E, Tisell L-E, Nilsson O, Fjälling M, Ahlman H. Intraoperative detection of somatostatin-receptor positive neuroendocrine tumors using ^{111}In-DTPA-Phe^1-octreotide. *Br J Cancer* 1996;73:770–775.
23. Kassis AI, Adelstein SJ, Sastry KSR. Kinetics of uptake, retention and radiotoxicity of ^{125}IUdR in mammalian cells: Implications of localized energy deposition by Auger processes. *Radiat Res* 1987;109:78–89.
24. Kassis AI, Adelstein SJ, Howell RW, Sastry KSR. Positional effects of Auger decays in mammalian cells in culture. In: Baverstock KF, Charlton DE, eds. *DNA damage by Auger emitters*. London: Taylor & Francis: 1988:1–13.
25. Rao DV, Mylavarapu VB, Sastry KSR, Howell RW. Internal Auger emitters: Effects on spermatogenesis and oogenesis in mice. In: Howell RW, Venkat RN, Sastry KSR, Rao DV, eds. *Biophysical aspects of Auger processes*. New York: AAPM: 1991:15–25.
26. Kassis AI, Fayad F, Kinsey BM, Sastry KSR, Adelstein SJ. Radiotoxicity of an ^{125}I-labeled DNA intercalator in mammalian cells. *Radiat Res* 1989;118:283–294.
27. Warters RL, Hofer KG, Harris CR, Smith JM. Radionuclide toxicity in cultured mammalian cells: elucidation of the primary site of radiation damage. *Curr Topics Radiat Res* 1977;12:389–407.

Temporal Changes in Function and Regional Glucose Uptake within Stunned Porcine Myocardium

Edward O. McFalls, Douglas Baldwin, David Marx, Peggy Fashingbauer and Herbert Ward
Cardiovascular Division, VA Medical Center, University of Minnesota, Minneapolis, Minnesota

This study compared the effects of porcine myocardial stunning on the uptake of [^{18}F]-fluorodeoxyglucose (FDG) at 24 hr and 7 days after reperfusion. Prior studies in animals subjected to severe myocardial ischemia have shown a sustained increase in FDG uptake relative to perfusion (FDG/MBF). The time course of recovery of FDG/MBF relative to function poststunning, however, has not been well characterized. **Methods:** Stunning was induced in eight swine by partially occluding the LAD artery for 20 min. At 1 and 7 days postreperfusion, function was assessed by two-dimensional echocardiography and PET studies were obtained with FDG and either ^{15}O-water or ^{13}N-ammonia. Blood flow by microspheres was determined at baseline, during ischemia and after stunning. Myocardial uptake of FDG relative to blood flow on matching images (FDG/MBF) was calculated for all ROIs and expressed as a ratio of LAD to non-LAD areas. **Results:** After stunning, left ventricular ejection fraction (LVEF) increased from 42% ± 10% on Day 1 to 52% ± 6% on Day 7 ($p < 0.05$). At Day 1, myocardial blood flow was 0.60 ± 0.10 ml/min/g in LAD and 0.67 ± 0.16 in non-LAD regions and neither differed at Day 7. The magnitude of FDG/MBF in the LAD region when normalized to the non-LAD region was 1.29 ± 0.16 on Day 1 and 1.09 ± 0.08 on Day 7 ($p < 0.05$) and was inversely proportional to global measures of LVEF ($r^2=0.61$; $p < 0.005$). **Conclusion:** The severity of postischemic LV dysfunction at 1 and 7 days after stunning correlates with the degree of enhanced regional glucose uptake as estimated by PET. Both normalize within 7 days, suggesting that metabolic and functional abnormalities within completely reperfused myocardium recover in parallel.

Key Words: PET; myocardial stunning; myocardial ischemia; reperfusion injury; glucose uptake; fluorine-18-FDG

J Nucl Med 1996; 37:2006–2010

Received Dec. 11, 1995; revision accepted Apr. 5, 1996.
For correspondence or reprints contact: Edward O. McFalls, MD, PhD, Division of Cardiology, University of Minnesota-VA Medical Center, 1 Veterans Dr., Minneapolis, MN 55417.

Imaging of the heart with PET can detect underperfused but metabolically active myocardium. Enhanced uptake of the glucose analog [^{18}F]fluorodeoxyglucose (FDG) within hypoperfused regions has been termed a flow-metabolism mismatch and is 70%–80% predictive of the return of regional function after coronary artery revascularization (*1,2*). In patients who have had a recent myocardial infarction, FDG uptake may also be increased within stunned regions, but the return of function occurs primarily within normally perfused segments (*3,4*). Although normalization of blood flow is the primary determinant of functional recovery after stunning, knowledge of the time course of metabolic recovery within reperfused myocardium allows the clinician to assess whether patients with a recent myocardial infarction can tolerate subsequent demands on the heart.

PET studies in animals have identified important temporal changes in myocardial blood flow, glucose uptake and oxygen consumption after severe ischemia and reperfusion. Within stunned myocardium, enhanced glucose uptake relative to blood flow may not be evident immediately after reperfusion but can be detected 24 hr and longer after the ischemic event (*5–7*). Oxygen consumption, as measured by the decay of ^{11}C-acetate and fatty acid utilization using ^{11}C-palmitate, may also be abnormal after ischemia (*8–10*), but, along with function, recovers within 2 wk (*10*). Although there is some evidence that FDG uptake normalizes by 4 wk of reperfusion, the relationship between glucose uptake and function within stunned myocardium has not been well characterized.

Accordingly, the aim of this study was to relate postischemic changes in function with FDG uptake relative to perfusion (FDG/MBF) after 20 min of ischemia. This degree of ischemia is too brief to induce inflammation that could confound the interpretation of enhanced FDG uptake in postischemic regions (*11*). We postulated that the ratio of FDG uptake to perfusion